GLIA 56:342–353 (2008)

Spontaneous Na^+ Transients in Individual Mitochondria of Intact Astrocytes

GUILLAUME AZARIAS,[1] DIMITRI VAN DE VILLE,[2] MICHAEL UNSER,[2] AND JEAN-YVES CHATTON[1,3,4]*
[1]*Department of Physiology, University of Lausanne, Switzerland*
[2]*Biomedical Imaging Group, Swiss Institute of Technology, Lausanne, Switzerland*
[3]*Department of Cell Biology and Morphology, University of Lausanne, Switzerland*
[4]*Cellular Imaging Facility, University of Lausanne, Switzerland*

KEY WORDS
glia; sodium; calcium; mitochondrial potential; fluorescence microscopy; ATP; neurons

ABSTRACT
Mitochondria in intact cells maintain low Na^+ levels despite the large electrochemical gradient favoring cation influx into the matrix. In addition, they display individual spontaneous transient depolarizations. We report here that individual mitochondria in living astrocytes exhibit spontaneous increases in their Na^+ concentration (Na^+_{mit} spiking), as measured using the mitochondrial probe CoroNa Red. In a field of view with ~30 astrocytes, up to 1,400 transients per minute were typically detected under resting conditions. Na^+_{mit} spiking was also observed in neurons, but was scarce in two nonneural cell types tested. Astrocytic Na^+_{mit} spikes averaged 12.2 ± 0.8 s in duration and 35.5 ± 3.2 mM in amplitude and coincided with brief mitochondrial depolarizations; they were impaired by mitochondrial depolarization and ruthenium red pointing to the involvement of a cation uniporter. Na^+_{mit} spiking activity was significantly inhibited by mitochondrial Na^+/H^+ exchanger inhibition and sensitive to cellular pH and Na^+ concentration. Ca^{2+} played a permissive role on Na^+_{mit} spiking activity. Finally, we present evidence suggesting that Na^+_{mit} spiking frequency was correlated with cellular ATP levels. This study shows that, under physiological conditions, individual mitochondria in living astrocytes exhibit fast Na^+ exchange across their inner membrane, which reveals a new form of highly dynamic and localized functional regulation.

INTRODUCTION

Mitochondria have the crucial function of producing ATP via oxidative phosphorylation (Mitchell, 1979). They are also known to be important regulators of cellular functions such as Ca^{2+} homeostasis and death pathways (Demaurex and Distelhorst, 2003; Nicholls and Budd, 2000). They can be addressed to specialized cellular domains (Reynolds and Rintoul, 2004) and have been shown to be in close interaction with subcellular organelles such as the endoplasmic reticulum and sub-plasmalemal compartments (Montero et al., 2000; Rizzuto et al., 1998; Walter and Hajnoczky, 2005). Even though the basic postulates of the chemiosmotic coupling hypothesis include an inner mitochondrial membrane with low permeability to cations (Mitchell, 1979), it is now admitted that the inner membrane contains channels and transporters with diverse selectivity for K^+ and Na^+ (Bernardi, 1999). Indeed regulatory mechanisms enable mitochondria to maintain both volume and cation content under control despite the extreme electronegativity of mitochondrial matrix would be sufficient to bring the concentration of monovalent cations such as Na^+ to molar range (Bernardi, 1999).

The isolated mitochondria model has provided a vast amount of information on mitochondrial transport of cations using kinetics measurements of the matching volume changes assessed with optical methods. More recently, with the availability of fluorescent probes selective for mitochondria and of sensitive imaging methods, the study of mitochondria in their native cellular environment has become possible. It includes the monitoring of mitochondrial electrical potential, pH and calcium concentration (e.g., Pinton et al., 2007). Such tools have permitted to establish that Ca^{2+} plays critical roles in mitochondrial physiology through the control of key mitochondrial enzymes such as Ca^{2+}-sensitive dehydrogenases, linking cellular Ca^{2+} homeostasis with metabolism (Hajnoczky et al., 1995). In addition, several studies report that mitochondria under physiological conditions exhibit spontaneous changes in their electrical membrane potential in neural (Buckman and Reynolds, 2001) and nonneural cells (Duchen et al., 1998).

Until recently, the dynamics of mitochondrial Na^+ (Na^+_{mit}) content has remained unexplored because of the lack of adequate methods. However, Na^+_{mit} is likely to play both direct and indirect roles in mitochondrial physiology. Its most recognized function is to drive the mitochondrial Na^+/Ca^{2+} antiporters that extrude Ca^{2+} ions from the mitochondrial matrix (Jung et al., 1992,

This article includes supplementary video clips available via the Internet at http://www.interscience.wiley.com/jpages/0894-1491/suppmat.

Grant sponsor: Swiss National Science Foundation; Grant number: 3100A0-108395.

*Correspondence to: Dr. Jean-Yves Chatton, Department of Cell Biology and Morphology, University of Lausanne, Rue du Bugnon 9, CH-1005 Lausanne, Switzerland.
E-mail: jean-yves.chatton@unil.ch

Received 20 October 2007; Accepted 23 November 2007

DOI 10.1002/glia.20619

Published online 20 December 2007 in Wiley InterScience (www.interscience.wiley.com).

1995). Na^+ has also been reported to modulate the activity of mitochondrial enzymes such as oxoglutarate and pyruvate dehydrogenase by decreasing their sensitivity to Ca^{2+} (Denton et al., 1980). Evidence also exists for a direct action of Na^+ on the activity of the pyruvate dehydrogenase complex by conformational changes (Pawelczyk and Olson, 1995). In addition, Na^+_{mit} has been reported to exhibit significant changes during cellular responses. For instance, afferent synaptic stimulation was shown to increase Na^+_{mit} concentration in hippocampal neurons (Pivovarova et al., 2002). We recently showed that in living astrocytes, Na^+_{mit} concentration displays rapid increase as a result of plasma membrane Na^+-dependent glutamate uptake, one of the most prominent functions of astrocytes in the brain (Bernardinelli et al., 2006). Thus, it is of critical importance to determine whether Na^+ could significantly influence mitochondrial functions such as ATP production. Indeed, it is expected that selective change in Na^+_{mit} concentration could alter the homeostasis of Ca^{2+} and proton through its respective Na^+-coupled exchangers expressed at inner mitochondrial membrane.

In the present study, we demonstrate for the first time that individual mitochondria in resting cells display spontaneous and rapid transients of their Na^+ concentration. Using a dedicated image analysis strategy, we characterized this Na^+_{mit} spiking activity at the level of single mitochondria using the Na^+-sensitive fluorescent probe CoroNa Red (CR) and investigated the underlying mechanisms of generation and regulation. We identified mitochondrial cation uniporters and mitochondrial Na^+/H^+ exchanger as critically involved in Na^+ entry and recovery, respectively. Ca^{2+} was found to play a permissive role in the regulation of the activity. We also found evidence for a modulation of spiking activity by the cellular energy metabolic status, which could point to the functional significance of these highly localized subcellular ion movements.

MATERIALS AND METHODS

Cell Culture and Solutions

Cortical astrocytes in primary culture were prepared from 1 to 3-days-old C57 Bl 6 mice as described elsewhere (Sorg and Magistretti, 1992). Astrocytes were cultured for 3–4 weeks in DME medium (Sigma) plus 10% FCS before experiments. Mouse cortical neurons were prepared as described before (Morgenthaler et al., 2006). All cell types, including MIN-6 and MCF-7 cells, were plated on glass coverslips for imaging. Experimental solutions contained (mM) NaCl, 135; KCl, 5.4; $NaHCO_3$, 25; $CaCl_2$, 1.3; $MgSO_4$, 0.8; and NaH_2PO_4, 0.78. Ca^{2+}-free solution contained NaCl, 135; KCl, 5.4; $NaHCO_3$, 25; $MgSO_4$, 0.8; NaH_2PO_4, 0.78; and EGTA, 0.1; both were bubbled with 5% CO_2/95% air. Na^+-free solutions contained *N*-methyl-D-glucamine chloride, 160; KCl, 5.4; $CaCl_2$, 1.3; $MgSO_4$, 0.8; K_3PO_4, 0.78; and HEPES, 20 (pH 7.4) and were compared with corresponding Na^+-containing control solutions buffered with HEPES, both bubbled with air. The solution used to deliver BAPTA-AM (50 μM) to cells contained in addition 1 g % bovine serum albumin and was also buffered with HEPES. Unless otherwise indicated, experimental solutions contained 5 mM glucose as metabolic substrate. Solutions for dye-loading contained (mM) NaCl, 160; KCl, 5.4; HEPES, 20; $CaCl_2$, 1.3; $MgSO_4$, 0.8; NaH_2PO_4, 0.78; glucose, 20 and was supplemented with 0.1% Pluronic F-127 (Molecular Probes, Eugene, OR).

Fluorescence Imaging

Mitochondrial Na^+ concentration was investigated and calibrated as described by Bernardinelli et al. (2006). Briefly, astrocytes were loaded at 37°C for 18 min with 1 μM CR in a HEPES-buffered balanced solution and then placed in a thermostated chamber designed for rapid exchange of perfusion solutions (Chatton et al., 2000) and superfused at 35°C. Low-light level fluorescence imaging was performed on an inverted epifluorescence microscope (Axiovert 100M, Carl Zeiss) using a 40 × 1.3 N.A. oil-immersion objective lens. Fluorescence excitation wavelengths were selected using a monochromator (Till Photonics, Planegg, Germany) and fluorescence was detected using a 12-bit cooled CCD camera (Princeton Instruments). CR fluorescence was excited at 560 nm and detected at >580 nm. To avoid phototoxicity, excitation intensity was reduced to 10 μW (as measured at the entrance pupil of the objective) by means of neutral density filters. Image acquisition and time series were computer-controlled using the software Metafluor (Universal Imaging, Reading, PA) running on a Pentium computer. Two-minute sequences of images were recorded at 1.0 Hz during control and experimental conditions; images were also acquired at lower rate between experimental conditions. Simultaneous monitoring of Na^+_{mit} and mitochondrial electrical potential were performed using CR (1 μM) and JC-1 (1–2 μM), loaded together for 17 min and imaged by confocal microscopy (SP5 Resonant scanner, Leica Microsystems) using excitation light at 561 and 488 nm, respectively. Dye emissions were observed at 580–620 nm (CR and JC-1 aggregates) and 500–560 nm (JC-1 monomers). Intracellular pH measurement was performed using the pH-sensitive dye BCECF-AM as described previously (Chatton et al., 2001), in some cases co-loaded with CR. ATP levels were assessed indirectly by measuring intracellular free Mg^{2+} using Magnesium Green AM as described previously (Chatton and Magistretti, 2005).

Image Analysis

To quantify the CR signal transients in a reliable and efficient way, we developed a dedicated image analysis procedure. The complete algorithm is implemented in Java as a plug-in for the ImageJ software (W. Rasban, http://rsb.info.nih.gov/ij/). In what follows, we outline the important processing steps of the algorithm.

First, we make use of the wavelet transform (Mallat, 1989), which is a popular tool in many areas of signal and image processing (Unser and Aldroubi, 1996). The third degree Battle-Lemarié wavelet transform (Battle, 1987; Unser and Blu, 2000) is applied to the 2D + T (two spatial dimensions plus time) stack of images in a separable way (i.e., along each dimension). Note that the wavelet decomposition is a linear, one-to-one transform that is orthogonal. It can be interpreted as a subband decomposition whereby the signal is split into details at different scales in space and time. In Fig. 2A, we illustrate one decomposition level of the spatiotemporal transform. The various subbands are typically designated by the combination of lowpass (L) or highpass (H) filters along horizontal, vertical, and temporal dimensions; i.e., LLL, LLH, up to HHH. In the full transform, the low-pass subband (LLL) is then further decomposed. This multi-resolution decomposition of the stack of images allows us to separate features of specific spatial size and temporal duration by selecting appropriate subbands. We empirically identified the CR transient as being spatially clustered over at least 4 pixels in horizontal and vertical directions, and with a strong temporal correlation over at least four images. Once the corresponding subbands are selected, the inverse wavelet transform is computed. This operation can be interpreted as separating CR transient from the slowly varying background and the highly uncorrelated thermal noise from the CCD camera.

Secondly, the reconstructed 2D+T stack of images mainly containing CR transients is thresholded. The threshold value is computed as three times the standard deviation of the first highpass (spatial and temporal) subband of the wavelet decomposition. Note that this particular subband contains almost exclusively noise. Both the thresholded (intensity-preserved) and a binarized stacks of images are saved for further processing. The intensity-preserved stack is further summarized in a cumulative image (over time) to characterize the total signal intensity of the experimental condition (later named "Cumulative Intensity"). A paired stack that combines the untreated data and the detected transient is also generated and allows direct visual inspection of the performance of the algorithm. A high degree of correspondence of the extracted events and excellent sensitivity of detection was observed in routine.[1]

CR transients were analyzed in a square area of 160 μm × 160 μm of confluent astrocytes. Of the 120 images recorded at 1 Hz for each experimental condition, a stack of 64 consecutive images were extracted for analysis. The frequency of transients is presented in terms of "Spiking Frequency" as the total number of cluster counts detected in 64 consecutive images. For the analysis of Na^+_{mit} spiking mechanisms, as spiking frequencies varied among experiments, data are presented as percent ± SEM spiking frequency measured in control conditions. For each group of experiments, a Student's *t* test was performed to assess the statistical significance against respective controls and *, **, and *** refer to *P* values <0.05, 0.01, and 0.001, respectively.

[1]The algorithm developed for the wavelet-based extraction of mitochondrial spiking activity is available under the form of an ImageJ plug-in from the site http://bigwww.epfl.ch/jmitotransient/.

Materials

All used dyes were from Invitrogen-Molecular Probes. *p*-Trifluoromethoxy carbonyl cyanide phenyl hydrazone (FCCP), cyclosporin A, ouabain, BAPTA-AM, and rotenone were from Fluka (Buchs, Switzerland). Bongkrekic acid, CGP-37157 and U 37883A were from Biomol (ANAWA Trading, Zurich, Switzerland). CNQX and TBOA were from Tocris (ANAWA Trading). Ethyl-isopropyl amiloride was a gift from Dr. H. Lang (Aventis Pharma, Frankfurt, Germany). All other substances were from Sigma. S-nitroso-cysteine was freshly prepared according to Lei et al. (1992).

RESULTS

Individual Mitochondrial Na^+_{mit} Spiking

We previously showed that CR staining of living astrocytes was selective for mitochondria (Bernardinelli et al., 2006) as it was found for other cell types (Baron et al., 2005; Yang et al., 2004). CR can be safely used as a mitochondrial Na^+ sensitive fluorescent probe, as it was shown to be selective for Na^+ with no influence of pH, Ca^{2+}, or K^+ in their respective expected physiological ranges (Bernardinelli et al., 2006; Jayaraman et al., 2001a, b).

Mitochondria in cultured astrocytes appeared as morphologically heterogeneous organelles, with a perinuclear aggregation and a predominance of isolated mitochondria in the cell periphery as reported in other studies (Collins et al., 2002) (Fig. 1A). In primary culture, astrocytes exhibit a flat morphology making the resolution of individual mitochondria possible even with a nonconfocal optical system. In CR-labeled astrocytes, we have repeatedly observed the presence of spontaneous CR transients. Figure 1A depicts a dynamic image sequence and shows individual mitochondria spontaneously lighting up (see also Movie 1; provided in supplementary material). CR transients were invariably seen in all the performed experiments (total >150 exp) apparently randomly distributed in space and time throughout the cell. Initial controls indicated that transients could be observed during superfusion of experimental solutions and in stationary media; in bicarbonate/CO_2 and in HEPES-buffered saline (not shown). Long-term recordings indicated that virtually all mitochondria of a cell displayed at least one CR transient during a 20-min period, excluding that transients were restricted to a subpopulation of mitochondria (not shown). Individual mitochondria usually showed 1–2 transients in 2-min periods of recording (Fig. 1B). The analysis of fluorescence changes in individual mitochondria indicated that the duration of one transient was found to be 12.2 ± 0.8 s

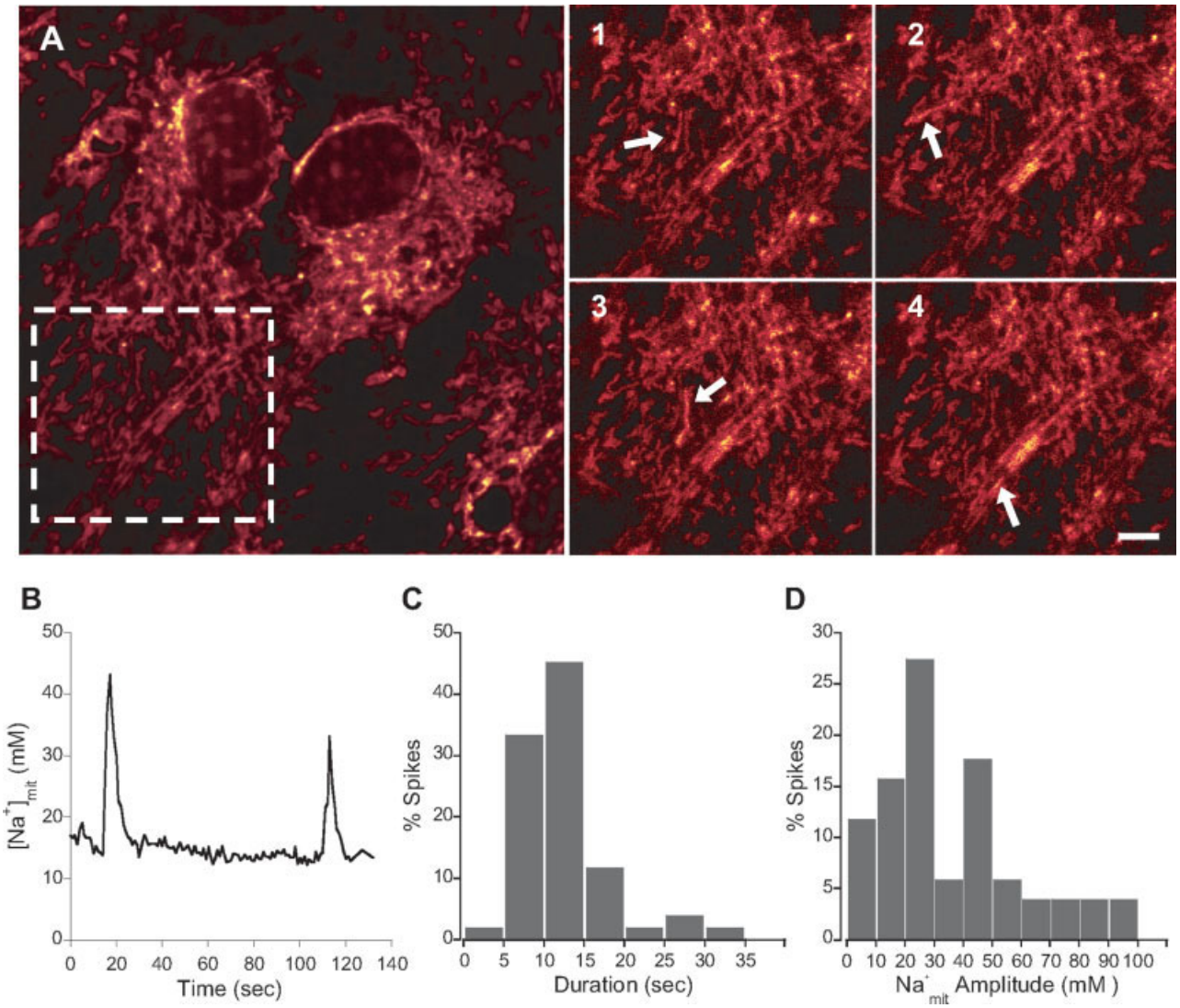

Fig. 1. Na^+_{mit} spiking in individual mitochondria. (**A**) Confocal fluorescent images of CR-stained astrocytes showing typical mitochondrial loading pattern. Blown up views (1–4) show a sequence of images recorded at low light level showing CR fluorescence transients in individual mitochondria. Images were taken at t = 0, 7.0, 11.7, and 13.0 s. Several Na^+_{mit} signal transients are indicated with arrows. Scale bar, 5 μm. (**B**) Trace of calibrated Na^+_{mit} changes recorded in one single mitochondrion which exhibited two Na^+_{mit} spikes during the recording period. (**C**, **D**) Distribution of the duration and amplitude of Na^+_{mit} spikes. Results from a total of 51 mitochondrial transients pooled from seven calibration experiments. Data are reported as percent of the total number of analyzed spikes. [Color figure can be viewed in the online issue, which is available at www. interscience.wiley.com.]

(median: 11.9 s; Fig. 1C). Calibration of mitochondrial Na^+ indicated that basal Na^+_{mit} was 13 ± 0.6 mM and the amplitude of transients averaged 35.5 ± 3.2 mM (median: 27.3 mM; Fig. 1D). The rate of Na^+_{mit} change during spiking was estimated at 12.3 ± 2.4 mM/s and 5.2 ± 0.7 mM/s for influx and efflux, respectively. In this report, we refer to CR transients in individual mitochondria as Na^+_{mit} spiking.

Given the large number of Na^+_{mit} spikes observable in an image sequence (>100 spikes/min in the field of view of 160 μm × 160 μm corresponding to about 30 confluent astrocytes), it rapidly became obvious that, to obtain a reliable and unbiased assessment of the Na^+_{mit} spiking activity, we had to use a dedicated image analysis strategy. Therefore, they developed an image analysis algorithm based on the wavelet transform. From consecutive images recorded at 1 Hz, this algorithm produces a sparse representation of the data in the spatial and frequency domain (Fig. 2A and refer to the section Materials and Methods). The algorithm includes a spatio-temporal filter excluding an effect of mitochondrial small movements on the detection. As a result, we obtained for each image in the sequence the average number of events, later used for spiking frequency assessment. The cumulative intensity of the transients detected reflects a combined evaluation of frequency and strength of transients. Figure 2B shows an example of analysis for an individual image. In control conditions, the sum of detected spikes number increased linearly over time in a field of view (R^2 > 0.995 for seven calibration experi-

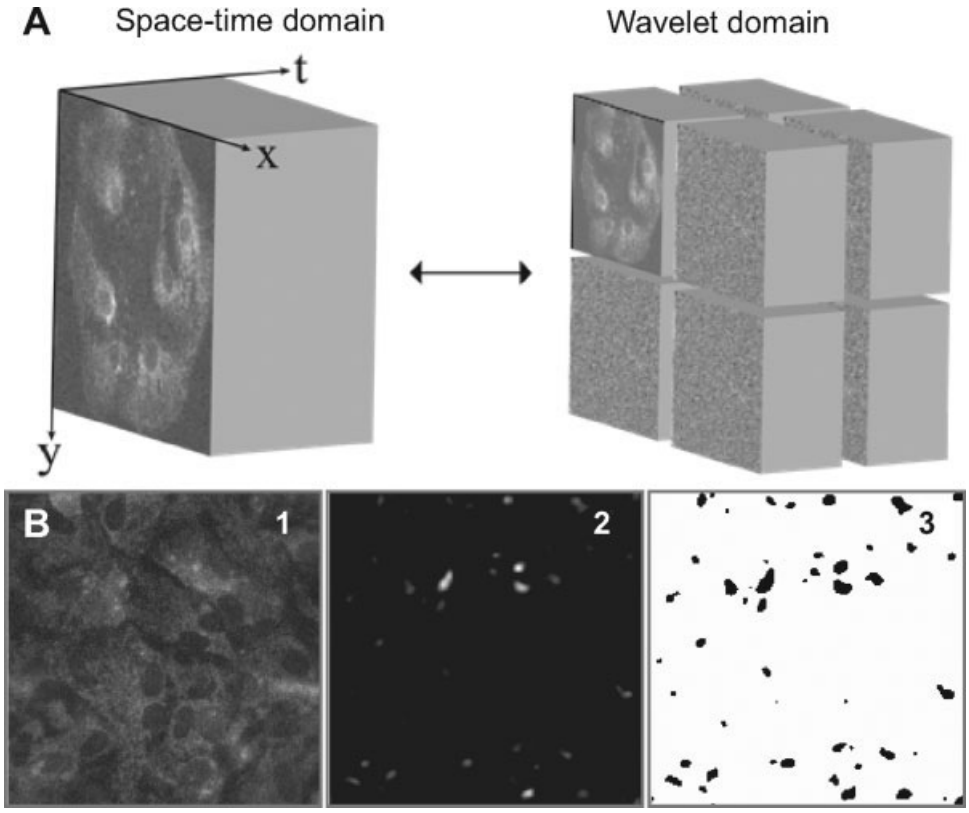

Fig. 2. Quantification of Na^+_{mit} spiking. (**A**) Illustration of the spatiotemporal wavelet transform (one decomposition level) applied to the series of images on the left. The transform is linear, nonredundant, and orthogonal. The full transform further decomposes the lowpass subband. (**B**) The image analysis method for a single raw image of cells loaded with CR with several brighter spots indicative of a Na^+_{mit} spike (B1) isolates transients but preserves intensities (B2); these are used for cumulative intensity measurements of spiking activity on the whole image sequence. Cluster analysis of binarized results (B3) is then applied to the entire image sequence to assess the frequency of Na^+_{mit} spiking.

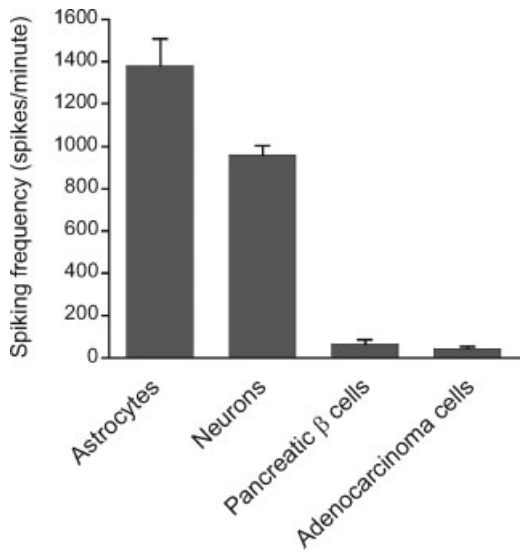

Fig. 3. Comparison of Na^+_{mit} spiking in different cell types. Spiking activity was compared between astrocytes, cortical neurons, and nonneural cells, namely pancreatic β cells (MIN-6 cell line) and mammary adenocarcinoma cells (MCF-7 cell line). Data are mean number (± SEM) of detected spikes per field per minute from $n = 156$ (astrocytes), 4 (neurons), 3 (MIN-6 cells), and 6 (MCF-7 cells) experiments.

ments, not shown). Spiking activity was thus rather steady and did not display bursting-like behavior.

Using this quantification tool, we then asked whether Na^+_{mit} spiking was a mitochondrial behavior found in all cell types. The presence of Na^+_{mit} spiking was investigated in mouse primary cortical neurons, in MIN-6 cells (mouse pancreatic β cell line), in MCF-7 cells (human mammary adenocarcinoma cell line), and compared with mouse cortical astrocytes under identical conditions. This analysis revealed that whereas both neural cell types exhibited robust Na^+_{mit} spiking, both MIN-6 cells and MCF-7 showed only marginal signs of Na^+_{mit} spiking (Fig. 3).

Collectively, this set of experiments indicated that the manifestation of Na^+_{mit} spiking is vastly different among cell types, which led us to consider Na^+_{mit} as a functional behavior of individual mitochondria. We therefore investigated the underlying pathways involved Na^+_{mit} spiking and focused our investigations in astrocytes.

Mechanisms Involved in the Generation of Na^+_{mit} Spiking

To determine which mechanisms and pathways are involved in Na^+_{mit} spiking, compounds described as

TABLE 1. Pathways Tested for Their Influence on Na^+_{mit} Spiking

Pathway	Drug	Cumulative mean intensity (% control)[a]	Spiking frequency (% control)[a]	*n*
NADH pathway—Complex I	Rotenone (1 μM)	100 ± 8	101 ± 3	7
Permeability transition pore	Bongkrekic acid (10 μM)	124 ± 30	116 ± 13	4
	Cyclosporin A (5 μM)	104 ± 24	114 ± 8	4
Adenine nucleotide transporter	Atractyloside (5 μM)	94 ± 36	107 ± 15	4
Mitochondrial K_{ATP} channel	U 37883A (100 μM)	113 ± 14	111 ± 1	2
	Diazoxide (100 μM)	146 ± 32	116 ± 12	15
Nitric oxide	S-nitroso-cysteine (200 μM)	102 ± 32	99 ± 5	2
Mitochondrial Na^+-Ca^{2+} exchanger	CGP-37157 (10 μM)	128 ± 44	120 ± 8	4
Mitochondrial H^+-K^+ exchanger	Quinine (100 μM)	125 ± 31	103 ± 13	6
Plasma membrane glutamate transporters	TBOA (500 μM)	103 ± 20	98 ± 6	6
AMPA/kainate receptors	CNQX (50 μM)	85 ± 17	91 ± 15	6

[a]Data are given as percent of control ±SEM; *n*, number of individual experiments. None of the listed compounds had a significant influence on Na^+_{mit} spiking activity ($P > 0.07$).

pharmacological blockers or modulators of mitochondrial conductances and transporters were tested. Those included CGP-37157, an inhibitor of mitochondrial Na^+/Ca^{2+}; quinine, inhibitor of the nonselective Na^+/H^+ (K^+/H^+) antiporter; rotenone, inhibitor of complex I of the mitochondrial respiratory chain; cyclosporine A and bongkrekic acid, blockers of the mitochondrial permeability transition pore; atractyloside, a blocker of adenine nucleotide translocator; U 37883A and diazoxide, blocker and opener of mitochondrial K_{ATP} channels, respectively; S-nitrosocysteine, a nitric oxide donor. A possible link with tonic glutamate release and subsequent reuptake or receptor activation was also tested: Na^+-glutamate transporters were inhibited using the specific inhibitor TBOA and non-NMDA receptors were blocked using 6-cyano-7-nitroquinoxaline-2,3-dione (CNQX). None of these maneuvers was found to decrease or increase spiking activity in a reproducible manner (Table 1).

To test for the involvement of mitochondrial cation uniporters, we used the blocker ruthenium red, acting both at the level of mitochondrial Ca^{2+} (Kirichok et al., 2004) and Na^+ uniporters (Kapus et al., 1990). Ruthenium red strongly decreased the overall Na^+_{mit} spiking activity (Fig. 4A). This compound did not alter the overall Na^+_{mit} level during the experiment, but caused a slight decrease in mitochondrial Ca^{2+} level (not shown). As a Na^+ influx through cation uniporters should be electrogenic, we performed simultaneous monitoring of Na^+_{mit} and mitochondrial electrical potential ($\Delta\Psi_{mit}$) using CR and JC-1, respectively. Mitochondria with highly negative membrane potential promote the formation of JC-1 dye aggregates, which fluoresce red; mitochondria with low potential will contain monomeric JC-1 and fluoresce green. Therefore, mitochondrial depolarization should lead to reversible increased green and decreased red emission, respectively. When loaded alone in astrocytes, JC-1 signals displayed spontaneous transient increases in the green channel whose kinetic was consistent with Na^+_{mit} spikes. JC-1 green transients were accompanied by corresponding decreases in the red channel (aggregates) only in the less frequent cases of longer lasting transients (4 events out of 21). Therefore, Na^+_{mit} spikes detected with CR emitting in the red channel, should not be confounded with JC-1 signals. Moreover, when loaded alone, CR reported Na^+_{mit} spiking in the red channel as expected, but caused no change in the green channel (not shown). We found that ~90% of detected Na^+_{mit} spikes (181 out of 199 spikes) were accompanied by corresponding rapid $\Delta\Psi_{mit}$ depolarizations observed in the green JC-1 fluorescence channel (Fig. 4B). Nevertheless, Na^+_{mit} spikes with no or barely detectable changes in $\Delta\Psi_{mit}$ were observable in a low number of events (not shown). Analysis of coincident Na^+_{mit} and $\Delta\Psi_{mit}$ spikes indicated that the onset of depolarizations started 0.45 ± 0.06 s ($n = 177$ analyzed events, $P < 0.001$) after the onset of Na^+_{mit} spikes. The depolarization transient reached its maximum 2.17 ± 0.13 s ($P < 0.001$) after the Na^+_{mit} spike maximum. It is unclear whether the observed delays reflect a lag between changes of Na^+_{mit} and potential, or is caused by a differential reactivity of the two fluorescent probes. The existence of this delay is another indication that there is no crosstalk between the two fluorescent signals. Surprisingly, experiments performed under similar conditions using the mitochondrial potentiometric dye rhodamine 123 (1 μM) did not reveal simultaneous depolarizations (not shown). The discrepancy can probably be explained by a difference in the sensitivity of the two probes; the amplitude of depolarization could have been too small or fast to be detectable by rhodamine 123, or the resting $\Delta\Psi_{mit}$ was too negative to lead to significant transmembrane dye movement (Ubl et al., 1996). Alternatively, there are indications that rhodamine 123 induce photodamage that impede spontaneous mitochondrial depolarization in neurons (Buckman and Reynolds, 2001), which could explain the observed differences. Finally, applying the mitochondrial uncoupler FCCP at low concentrations (0.01 and 0.05 μM), thereby weakening the driving force of the mitochondrial cation uniporter, diminished the frequency of CR transients (Fig. 4C). Taken together, these data suggest that mitochondrial cation uniporters are the Na^+ entry pathway during spiking.

In a previous study, we showed that the selective mitochondrial Na^+/H^+ exchanger is the main mechanism enabling the regulation of Na^+_{mit} concentration in astrocytes (Bernardinelli et al., 2006). This exchanger uses the proton (pH) gradient across the inner membrane to drive Na^+ out of the matrix. Involvement of this anti-

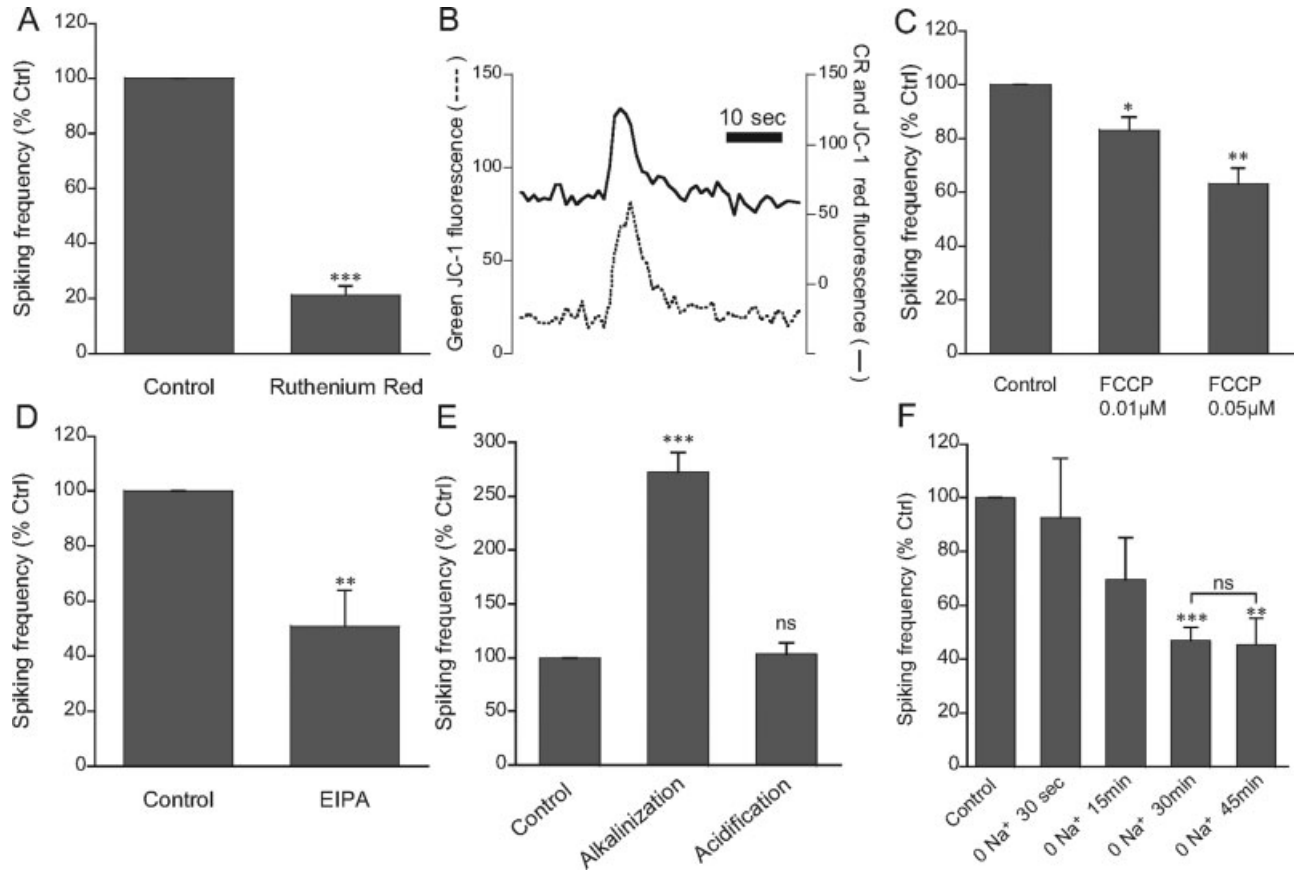

Fig. 4. Involvement of mitochondrial cation uniporters and mitochondrial Na^+/H^+ exchanger in Na^+_{mit} spiking. (**A**–**C**) Involvement of the mitochondrial cation uniporter. (A) After a control period, application of the uniporter blocker ruthenium red (50 µM) for 15 min strongly decreased Na^+_{mit} frequency ($n = 5$). Data are shown as percent of control ± SEM (B) Simultaneous Na^+_{mit} and $\Delta\Psi_{mit}$ measurements in individual mitochondria. The graph shows an example of mitochondrion exhibiting a Na^+_{mit} spike measured using CR (plain line, right axis) that was accompanied by a depolarizing transient measured using JC-1 in the green channel (dotted line, left axis). Experimental procedure is detailed in supplementary information. (C) Weakening of $\Delta\Psi_{mit}$ using the mitochondrial uncoupler FCCP decreased Na^+_{mit} spiking frequency ($n = 5$). (**D**, **E**) Involvement of the mitochondrial Na^+/H^+ exchanger. (D) Cells were perfused with the inhibitor of Na^+/H^+ exchanger EIPA (50 µM, $n = 5$), which decreased the spiking frequency. (E) Cytosolic alkalinization using a CO_2-free buffer ($n = 6$) dramatically increased the spiking frequency whereas intracellular acidification induced by ammonium pulse (20 mM, $n = 5$) did not alter the spiking frequency. (**F**) After a measurement in control condition, cells were perfused in Na^+-free solution (0 Na^+) and spiking frequency was measured at indicated time points ($n = 6$–10). Data are percent of respective controls ± SEM; ns, nonsignificant; $^*P < 0.05$; $^{**}P < 0.01$; $^{***}P < 0.001$ using a paired *t*-test.

porter for Na^+_{mit} spiking was then investigated. Five minutes superfusion of the inhibitor of mitochondrial Na^+/H^+ exchanger ethyl-isopropyl amiloride (EIPA) markedly decreased the Na^+_{mit} spiking frequency (Fig. 4D) without altering cytosolic pH as measured using the pH-sensitive fluorescent probe 2′,7′-bis-(2-carboxyethyl)-5-(and-6)-carboxyfluorescein acetoxymethyl ester (BCECF-AM) (not shown). The dependency of Na^+_{mit} spiking on cellular pH was then tested. Cellular alkalinization was accomplished by perfusion of a CO_2-free bicarbonate buffer, which increased the cell pH by 0.78 ± 0.02 units ($n = 4$ exp). This treatment strongly increased Na^+_{mit} spiking frequency (Fig. 4E). Acidification was obtained by introduction of an intracellular proton load following rapid washout of ammonium chloride. In this situation, pH decreased by 0.83 ± 0.02 units (30 cells, from 5 exp). This maneuver did not significantly alter Na^+_{mit} spiking frequency (Fig. 4E). The same result was obtained by mild acidification (0.07 ± 0.004 pH units, $n = 4$ exp) caused by application of the organic anion propionate (20 mM) that enters cells by nonionic diffusion (not shown). We then tested if the cellular Na^+ concentration could modulate the Na^+_{mit} spiking frequency. Astrocytes were first superfused with a Na^+-free solution. This treatment that lowers cellular Na^+ is expected to decrease Na^+_{mit} levels as well. As expected, under these conditions, both the overall Na^+_{mit} level and the amplitude of Na^+_{mit} spikes decreased gradually (not shown). However, the frequency of Na^+_{mit} spiking also declined significantly (Fig. 4F). Interestingly, the Na^+_{mit} spiking frequency reached a minimum at 30 min of Na^+ free solution perfusion and did not further decrease, whereas the cumulative mean intensity relative to spikes amplitude continued to drop. Conversely, we tested if Na^+_{mit} spiking frequency could be altered in increased Na^+_{mit} conditions. Induction of Na^+_{mit} increase by opening the K_{ATP} channel or by 5 min ouabain treatment (Bernardinelli et al., 2006) did not significantly enhance the Na^+_{mit} spiking activity (Table 1 and Fig. 6C). Thus, whereas Na^+_{mit} spiking activity was sensitive

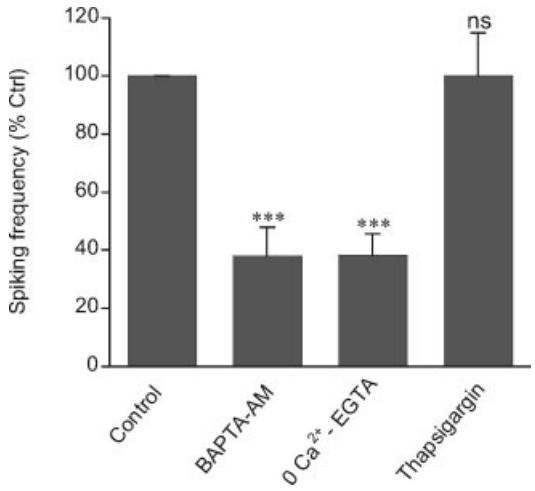

Fig. 5. Ca^{2+} plays a permissive role on Na^{+}_{mit} spiking activity. After a control period, BAPTA-AM (50 μM) was applied for 30 min after which Na^{+}_{mit} frequency was measured and showed a decrease in frequency ($n = 5$). Cell perfusion for 30 min with a Ca^{2+}-free solution (see Materials and Methods) decreased Na^{+}_{mit} spiking frequency by the same amount ($n = 5$). However, thapsigargin (1 μM) which induces an ER Ca^{2+} release did not alter spiking frequency ($n = 3$). Data are shown as percent of control ± SEM. (ns, nonsignificant; $^{***}P < 0.001$ using a paired *t*-test, compared with the control condition).

to lowered Na^{+}_{mit}, the spiking frequency was not correlated with cellular Na^{+} level above basal level. Taken together, this set of experiments emphasizes the involvement of mitochondrial Na^{+}/H^{+} exchangers as efflux pathways during Na^{+}_{mit} spiking.

Modulation of Na^{+}_{mit} Spiking Activity

We then looked into factors that could modulate Na^{+}_{mit} spiking activity. We first tested a role of intracellular Ca^{2+}, which was found to be involved in the glutamate-mediated increase of Na^{+}_{mit} level in astrocytes (Bernardinelli et al., 2006). In a first phase, cells were loaded with 1,2 bis(*o*-aminophenoxy)ethane-*N*,*N*,*N*′,*N*′-tetraacetic acid acetoxymethyl ester (BAPTA-AM) to chelate intracellular free Ca.$^{2+}$ Figure 5 shows that the frequency of Na^{+}_{mit} spiking was strongly diminished by chelating Ca^{2+}. In addition, decreasing cellular Ca^{2+} by superfusing astrocytes in a Ca^{2+}-free solution led to the same inhibition of Na^{+}_{mit} spiking activity (Fig. 5). However, acutely increasing cytosolic Ca^{2+} by endoplasmic reticulum (ER) Ca^{2+} release using thapsigargin did not cause an increase in Na^{+}_{mit} frequency. This set of experiments indicated that Ca^{2+} is involved in the regulation of Na^{+}_{mit} spiking.

We then explored the possible link between Na^{+}_{mit} spiking and cellular bioenergetics. In particular, ATP levels can undergo significant variations during activity in astrocytes. In these experiments, we applied maneuvers to manipulate cellular ATP and assessed the relative ATP level changes indirectly by measuring free Mg^{2+} using the fluorescent probe Magnesium Green as previously described (Chatton and Magistretti, 2005). As ATP hydrolysis releases bound Mg^{2+}, Magnesium Green fluorescence intensity is inversely related to cytosolic ATP concentration. To cause a severe ATP depletion, cells were treated with 2-deoxyglucose (2-DG) plus oligomycin, inhibitors of glycolysis and mitochondrial ATP synthase, respectively (Fig. 6A, left). To induce an intermediate ATP decrease, cells were superfused with the neurotransmitter glutamate (Fig. 6A, center). In astrocytes, the cellular uptake of glutamate significantly lowers ATP levels by strong stimulation of the Na,K-ATPase (Chatton and Magistretti, 2005; Chatton et al., 2000). Finally, to increase ATP levels, the Na,K-ATPase was inhibited using ouabain. The Na^{+} pump being a major ATP consumer in astrocytes (Chatton and Magistretti, 2005), its inhibition led to a transient increase in cellular ATP levels (maximal at ~30 s) which decreased close to baseline after 5 min (Fig. 6A, right). The relative ATP level changes caused by these maneuvers are summarized in Fig. 6B. In a second phase, the same experimental maneuvers were repeated on cells and Na^{+}_{mit} spiking was recorded. Figure 6C shows that Na^{+}_{mit} spiking frequency was influenced by maneuvers altering ATP levels and followed a positive correlation with the relative ATP level. ATP synthesis blockers impaired Na^{+}_{mit} spiking activity by 29%. However, this treatment was found in separate experiments to cause a mild mitochondrial depolarization (not shown). Glutamate, which, by its stimulation of Na,K-ATPase activity, decreased ATP levels to a lesser extent, also decreased Na^{+}_{mit} spiking activity. It is worthy of note that glutamate application did not depolarize mitochondria, rather slightly hyperpolarized them (not shown). Ouabain, inducing a transient increase in ATP level, which was maximal at 30 s, induced an increase in Na^{+}_{mit} spiking frequency. Collectively, these data suggest that the cellular ATP level could provide a feedback regulation on Na^{+}_{mit} spiking activity.

DISCUSSION

The present study shows that individual mitochondria in resting astrocytes exhibit rapid spontaneous Na^{+} concentration transients. This first demonstration of Na^{+}_{mit} activity has been made possible by the Na^{+}-sensitive probe CR that loads into the matrix of mitochondria in living cells. The calibrated resting Na^{+}_{mit} level in astrocytes (~12–20 mM) was found to be consistent with values estimated for mitochondria of neurons (Pivovarova et al., 2002). Na^{+}_{mit} spikes of individual mitochondria have substantial amplitude and well-defined kinetics, with spike duration homogeneous among different mitochondria, cover-slips and cell cultures. Although Na^{+}_{mit} changes in certain mitochondria reached high values during spiking—often three times the basal concentration—Na^{+}_{mit} transients did not appear to be transmitted to neighboring mitochondria as a wave, which suggests that mitochondria of astrocytes do not form a lumenally continuous network but are morphological and functional distinct units as reported in other studies (Collins

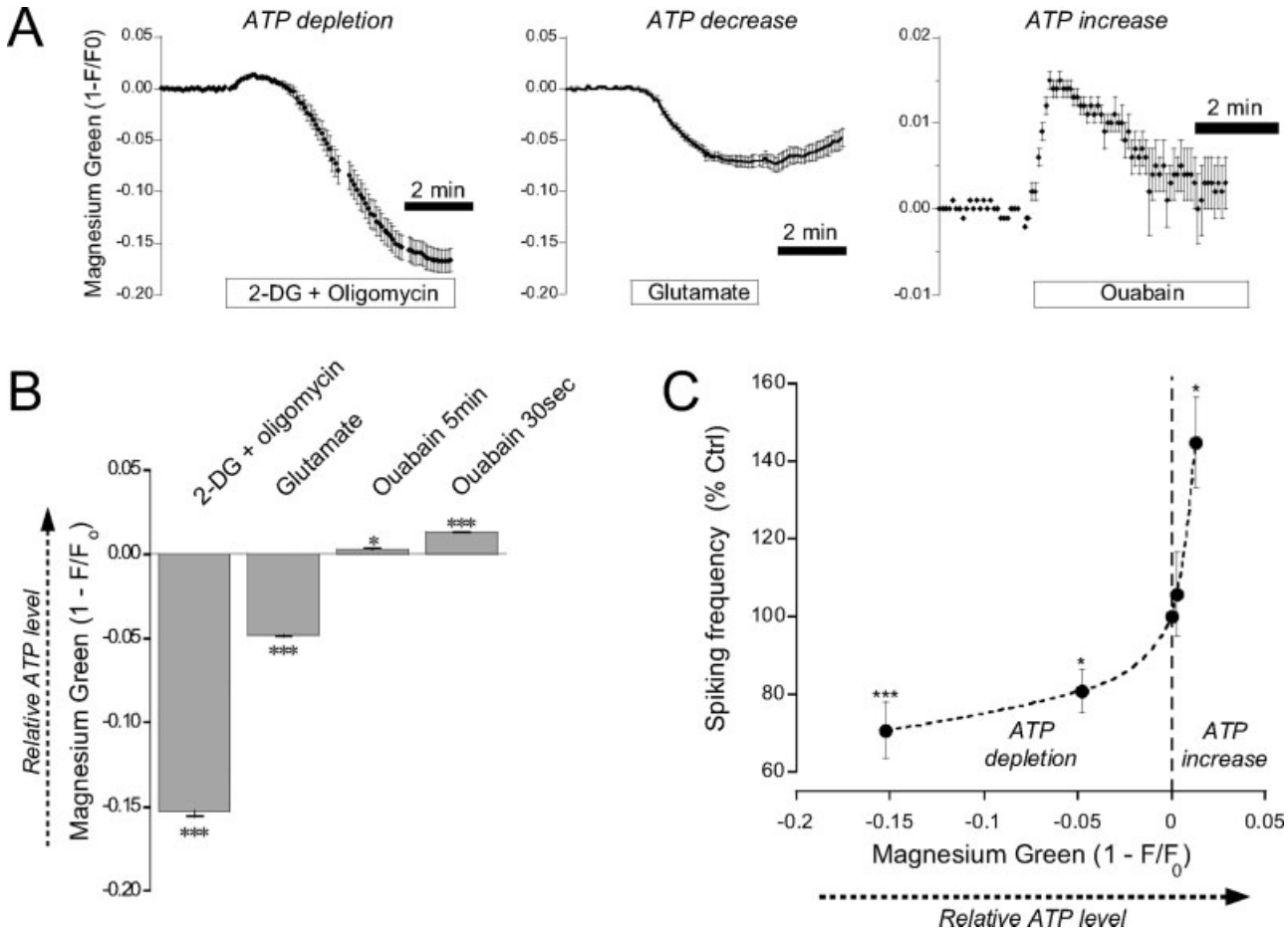

Fig. 6. Relationship between Na^+_{mit} spiking activity and cellular ATP levels. (**A**) Cellular ATP was depleted using 10 mM 2DG plus 1 μM oligomycin (left), or was decreased by glutamate (200 μM) application (center), or transiently increased by treatment of the cells with ouabain 1mM (right). The effectiveness of these maneuvers was assessed by monitoring relative ATP levels using Magnesium Green fluorescence changes. To make the data more legible, the fluorescence scale is shown as $1\text{-}F/F_0$, which is directly proportional with ATP levels. (**B**) Relative ATP levels during corresponding protocol shown in (A). Data are means ± SEM of three to four experiments for each protocol. (**C**) Using identical protocols, Na^+_{mit} spiking frequency was measured. The resulting spiking frequency was then plotted against the relative ATP levels summarized in (B) and showed a monotonical relationship between the two parameters. Spiking frequencies are presented as percent of control ± SEM from five to seven experiments for each protocol.

et al., 2002). During the recording period, stained mitochondria displayed no detectable morphological signs of fission or fusion linked to CR transients. Fission or fusion should result in similar change in other mitochondrial labeling. However, CR transients occurred without coincident alteration of rhodamine 123 staining, a mitochondrial selective dye. In addition, it has been recently reported that thapsigargin induces rapid Ca^{2+}-dependent fragmentation of mitochondria (Hom et al., 2007). Such treatment did not modify Na^+_{mit} spiking activity in our astrocyte preparation. Thus, it can be concluded that Na^+_{mit} spiking activity is a mitochondrial process distinct from fusion or fission. It is interesting to note that, whereas the nonneural cell types tested in our study (MIN-6 and MCF-7 cells) displayed a typical mitochondrial staining pattern, they exhibited a 21-fold and 31-fold lower Na^+_{mit} spiking activity, respectively, than astrocytes under identical experimental conditions. This observation could indicate that Na^+_{mit} spiking is preferentially expressed in cell types experiencing substantial intracellular Na^+ concentration changes during activity, such as neurons and astrocytes (Bernardinelli et al., 2004; Pivovarova et al., 2002).

To elucidate whether the driving force of Na^+ influx into mitochondria during spiking derives from the strongly negative potential across the inner membrane, we set up an experimental protocol to simultaneously record both Na^+_{mit} and $\Delta\Psi_{mit}$ and found that the vast majority of Na^+_{mit} spikes were accompanied with depolarizations of similar aspect. However both the onset and the peak of depolarization appeared to follow Na^+_{mit} changes with a certain lag. This lag is most probably due to differences in response kinetics of the two probes. Nevertheless, the coincidence and similar timecourse of $\Delta\Psi_{mit}$ and Na^+_{mit} signals are consistent with the notion that the electrophoretic Na^+ entry induces mitochondrial depolarization (Bernardi et al., 1990). The fact that such coincident depolarizations could not be detected using rhodamine 123, a potential-sensitive dye based on a different principle, probably indicates that the magnitude

of transient depolarizations was limited. In addition, the complete reversibility of both $\Delta\Psi_{mit}$ and Na^+_{mit} signals after spiking speaks against a complete collapse of potential. Assuming that mitochondrial depolarization was caused by Na^+_{mit} influx and considering that the involvement of the electrogenic Na^+/Ca^{2+} exchanger was excluded on the basis of the lack of effect of the inhibitor CGP-37157, the identity of the pathway for electrophoretic Na^+ entry appears to be a cation uniporter. Indeed Na^+_{mit} spiking activity was severely impaired by ruthenium red, a blocker of the mitochondrial Ca^{2+} and Na^+ uniporters (Kapus et al., 1990; Kirichok et al., 2004). Conversely, weakening of the driving force of the mitochondrial cation uniporter using the uncoupler FCCP diminished Na^+_{mit} spiking activity. Finally, the flux through the mitochondrial Na^+ uniporter was reported to display an optimum at alkaline pH (7.5–8), which is consistent with our observations of increased spiking activity at higher intracellular pH (Bernardi, 1999; Bernardi et al., 1990). Taken together, mitochondrial cation uniporters are realistic candidates for mediating Na^+ entry pathway during spiking.

The Na^+/H^+ exchanger of the inner mitochondrial membrane is described as the mechanism responsible for maintaining or restoring low Na^+_{mit} levels. We have recently shown that this transport system is critically involved in the regulation of Na^+_{mit} in astrocytes subjected to global intracellular Na^+ increase (Bernardinelli et al., 2006). An integrated model of Ca^{2+}, Na^+ and H^+ fluxes occurring in mitochondria during cardiac myocyte pacing activity recently showed that the Na^+ flux mediated by the Na^+/H^+ exchanger can reach 20 mM/s during pacing at 1–2 Hz (Nguyen et al., 2007). This value is higher than what found in our experiments during Na^+_{mit} spiking (5.2 ± 0.7 mM/s), making the Na^+/H^+ exchanger a plausible pathway involved during Na^+_{mit} spiking. The present report shows that inhibition of mitochondrial Na^+/H^+ exchanger strongly diminished Na^+_{mit} spiking activity. Other pieces of evidence point to a key role of this mechanism, namely the relationship with Na^+ and pH changes. In particular, the frequency of Na^+_{mit} spiking was found to be diminished by cellular Na^+ depletion. However, Na^+_{mit} spiking frequency was not correlated with Na^+_{mit} above basal level. For instance, ouabain treatment, which increases cytosolic as well as mitochondrial Na^+_{mit} levels, had a more pronounced effect on spiking frequency at 30 s when Na^+ levels are only increased by a few milimolar than after 5 min of ouabain application, when Na^+_{mit} levels have considerably increased (Bernardinelli et al., 2006). The Na^+/H^+ exchanger isoform NHE1 at the plasma membrane has an affinity for extracellular Na^+ of 3–50 mM (Putney et al., 2002), which means that because extracellular Na^+ concentration greatly exceeds these values, most exchangers operate under condition of saturation with respect to external Na^+ and under the driving force of the transmembrane Na^+ concentration. It might be a different situation in mitochondria, as the mitochondrial matrix Na^+ concentration was estimated to be in the range 12–18 mM in astrocytes (Bernardinelli et al., 2006) and where the driving force for Na^+/H^+ exchange is rather the transmembrane proton gradient. It is assumed that mitochondrial Na^+/H^+ exchangers display a Km of ~26 mM for Na^+ and are symmetrical in their interaction with Na^+ (Bers et al., 2003), with a consequence of being reversible. Another characteristic of the exchanger could also explain the observation that Na^+_{mit} spiking was strongly enhanced by cellular alkalinization. The corresponding exchanger at the plasma membrane is known to contain proton modifier sites, distinct from the proton transport site that critically controls the activity of transport (Wakabayashi et al., 2003). This was shown to be the case for three isoforms of the exchanger (NHE1, NHE2, and NHE3), and is likely to be also found in the mitochondrial isoform. Thus, in addition to cation uniporters (see above), the Na^+/H^+ exchanger could also underlie the observed effects of alkalinization both by a modulation of transporter turnover rate and by the alteration of pH gradients.

We found that Na^+_{mit} spiking activity was strongly affected by a decrease in calcium concentration, which indicated that Ca^{2+} appears to have a permissive role on spiking, although not through direct involvement of mitochondrial Na^+/Ca^{2+} exchangers. As mitochondria are in close interaction with ER (Rizzuto et al., 1998), we tested if Na^+_{mit} could be induced by spontaneous ER Ca^{2+} release as it was reported in cardiomyocytes (Duchen et al., 1998). Emptying the Ca^{2+} stores with thapsigargin had no effect on Na^+_{mit} spiking. In addition, astrocytes are known to display spontaneous cytosolic Ca^{2+} oscillations both in culture and in situ (Parri et al., 2001). However, these oscillations involve generalized cellular Ca^{2+} movements, very different from the localized Na^+_{mit} spikes observed here. Moreover, Ca^{2+} transients have threefold to fivefold longer duration than Na^+_{mit} spikes. Thus, it can be concluded that Na^+_{mit} spiking activity was not correlated with cellular Ca^{2+} oscillation, without excluding a potential long-term regulatory effect of Ca^{2+} oscillations.

As discussed earlier, several observations led us to conclude that increased cytosolic or mitochondrial Na^+ levels were not directly influencing Na^+_{mit} spiking frequency. For instance, glutamate application rapidly and substantially increases cytosolic and mitochondrial Na^+ concentrations in astrocytes, yet it decreased spiking frequency. These considerations led us to look into another element that could link these observations, namely ATP levels. Na^+-coupled glutamate uptake causes a substantial energy burden to astrocytes. The influx of Na^+ causes the Na^+ pump to more than double its activity, with corresponding increase in ATP hydrolysis (Chatton and Magistretti, 2005). Conversely, blocking the Na^+ pump, which accounts for about half of the total cellular ATP consumption in these cells, causes a sizable decreased ATP hydrolysis. Therefore we investigated to what extent cellular ATP levels, could be considered a factor influencing mitochondrial Na^+ spiking. Using a set of experimental maneuvers aimed at either decreasing or increasing ATP levels, we found indications that spiking was positively correlated with ATP

levels, which might indicate that ATP plays a modulatory or feedback role on Na^+_{mit} spiking. Several cellular elements could mediate such a modulation. For instance, a mitochondrial Na^+ permeable uniporter was described to be opened in low divalent cation containing medium and its open-state could be induced by ATP (Bernardi et al., 1990). Also, the activity of the Na^+/H^+ exchanger at the plasma membrane is known to be modulated by ATP (Demaurex et al., 1997; Wakabayashi et al., 2003).

Spontaneous mitochondrial depolarizations have been observed in neurons using the same mitochondrial potentiometric dye JC-1 used in our studies with astrocytes (Buckman and Reynolds, 2001). It is conceivable that a similar situation occurs in neurons and that Na^+_{mit} spikes could be at the origin of the observed mitochondrial depolarization. Taking the results of the present study together, we could speculate that mitochondrial depolarizations are driven by the opening of a mitochondrial cation uniporter in microdomains containing a high levels of ATP, inducing a substantial increase in Na^+_{mit} subsequently extruded by the mitochondrial Na^+/H^+ exchanger powered by the proton motive force. However, the experiments performed in this study do not allow discriminating between intra- and extramitochondrial ATP. As the existence of cytosolic ATP domains has been recently proposed to be unlikely (Barros and Martinez, 2007), mitochondrial ATP could be the triggering factor. Conversely, the activity of the mitochondrial Na^+/H^+ exchanger during Na^+_{mit} spiking, is expected to substantially alter pH in the mitochondrial matrix and intermembrane space, which could impact on the proton electrochemical gradient used by the ATP synthase. Thus, Na^+_{mit} spiking could have a modulatory role on mitochondrial energy production.

Finally, this first demonstration of spontaneous Na^+_{mit} spiking activity might reveal of critical importance for the understanding of astrocyte metabolism. First, intracellular Na^+ is a pivotal element in the bioenergetics of astrocytes enabling the coupling of neuronal activity and astrocyte metabolic response (Magistretti et al., 1999). In astrocytes, intracellular Na^+ is increasingly recognized as a factor critically involved in the regulation of energy metabolism, at the level of both intercellular and sub-cellular communication (Bernardinelli et al., 2004, 2006). Although astrocytes are electrically nonexcitable, they are subject to substantial variations in their cytosolic Na^+ concentration, as they are responsible for actively maintaining low extracellular levels of glutamate in the brain using the Na^+-coupled glutamate uptake (Danbolt, 2001). Astrocytes are known to favor aerobic glycolysis over oxidative phosphorylation as a response to enhanced glutamate uptake (Magistretti et al., 1999). Further work is needed to determine whether the decrease in Na^+_{mit} spiking frequency coincident with glutamate application is involved in the pattern of metabolic response of astrocytes, and whether spiking represents a form of frequency encoding of subcellular metabolic information, as proposed for Ca^{2+} oscillations in hepatocytes (Hajnoczky et al., 1995).

In conclusion, the present study shows that individual mitochondria in intact astrocytes display spontaneous transients of their Na^+ content. The underlying mechanisms of this spiking activity involve the activity of mitochondrial cation uniporters and mitochondrial Na^+/H^+ exchangers. Ca^{2+} was found to play a permissive role, whereas cellular ATP level a positive influence on Na^+_{mit} spiking activity.

ACKNOWLEDGMENTS

The authors gratefully acknowledge Corinne Moratal for her excellent technical assistance, Martin Jaeger for his help during the preliminary parts of the project, Igor Allaman, Yann Bernardinelli, Sabino Vesce for fruitful discussions and comments on the manuscript. They are indebted to N. Busso and R. Regazzi for providing MCF-7 and MIN-6 cells, respectively.

REFERENCES

Baron S, Caplanusi A, van de Ven M, Radu M, Despa S, Lambrichts I, Ameloot M, Steels P, Smets I. 2005. Role of mitochondrial Na^+ concentration, measured by CoroNa Red, in the protection of metabolically inhibited MDCK cells. J Am Soc Nephrol 16:3490–3497.

Barros LF, Martinez C. 2007. An enquiry into metabolite domains. Biophys J 92:3878–3884.

Battle G. 1987. A block spin construction of ondelettes. I. Lemarie functions. Commun Math Phys 110:601–615.

Bernardi P. 1999. Mitochondrial transport of cations: Channels, exchangers, and permeability transition. Physiol Rev 79:1127–1155.

Bernardi P, Angrilli A, Azzone GF. 1990. A gated pathway for electrophoretic Na^+ fluxes in rat liver mitochondria. Regulation by surface Mg^{2+}. Eur J Biochem 188:91–97.

Bernardinelli Y, Azarias G, Chatton J-Y. 2006. In situ fluorescence imaging of glutamate-evoked mitochondrial Na^+ responses in astrocytes. Glia 54:460–470.

Bernardinelli Y, Magistretti PJ, Chatton J-Y. 2004. Astrocytes generate Na^+-mediated metabolic waves. Proc Natl Acad Sci USA 101:14937–14942.

Bers DM, Barry WH, Despa S. 2003. Intracellular Na^+ regulation in cardiac myocytes. Cardiovasc Res 57:897–912.

Buckman JF, Reynolds IJ. 2001. Spontaneous changes in mitochondrial membrane potential in cultured neurons. J Neurosci 21:5054–5065.

Chatton J-Y, Idle JR, Vågbø CB, Magistretti PJ. 2001. Insights into the mechanisms of ifosfamide encephalopathy: Drug metabolites have agonistic effects on a-amino-3-hydroxy- 5-methyl-4-isoxazolepropionic acid (AMPA)/kainate receptors and induce cellular acidification in mouse cortical neurons. J Pharmacol Exp Ther 299:1161–1168.

Chatton J-Y, Magistretti PJ. 2005. Relationship between L-glutamate-regulated intracellular Na^+ dynamics and ATP hydrolysis in astrocytes. J Neural Transm 112:77–85.

Chatton J-Y, Marquet P, Magistretti PJ. 2000. A quantitative analysis of L-glutamate-regulated Na^+ dynamics in mouse cortical astrocytes: Implications for cellular bioenergetics. Eur J Neurosci 12:3843–3853.

Collins TJ, Berridge MJ, Lipp P, Bootman MD. 2002. Mitochondria are morphologically and functionally heterogeneous within cells. EMBO J 21:1616–1627.

Danbolt NC. 2001. Glutamate uptake. Prog Neurobiol 65:1–105.

Demaurex N, Distelhorst C. 2003. Cell biology. Apoptosis—The calcium connection. Science 300:65–67.

Demaurex N, Romanek RR, Orlowski J, Grinstein S. 1997. ATP dependence of Na^+/H^+ exchange. Nucleotide specificity and assessment of the role of phospholipids. J Gen Physiol 109:117–128.

Denton RM, McCormack JG, Edgell NJ. 1980. Role of calcium ions in the regulation of intramitochondrial metabolism. Effects of Na^+, $Mg2^+$ and ruthenium red on the $Ca2^+$-stimulated oxidation of oxoglutarate and on pyruvate dehydrogenase activity in intact rat heart mitochondria. Biochem J 190:107–117.

Duchen MR, Leyssens A, Crompton M. 1998. Transient mitochondrial depolarizations reflect focal sarcoplasmic reticular calcium release in single rat cardiomyocytes. J Cell Biol 142:975–988.

Hajnoczky G, Robbgaspers LD, Seitz MB, Thomas AP. 1995. Decoding of cytosolic calcium oscillations in the mitochondria. Cell 82:415–424.
Hom JR, Gewandter JS, Michael L, Sheu SS, Yoon Y. 2007. Thapsigargin induces biphasic fragmentation of mitochondria through calcium-mediated mitochondrial fission and apoptosis. J Cell Physiol 212:498–508.
Jayaraman S, Joo NS, Reitz B, Wine JJ, Verkman AS. 2001a. Submucosal gland secretions in airways from cystic fibrosis patients have normal [Na^+] and pH but elevated viscosity. Proc Natl Acad Sci USA 98:8119–8123.
Jayaraman S, Song Y, Vetrivel L, Shankar L, Verkman AS. 2001b. Noninvasive in vivo fluorescence measurement of airway-surface liquid depth, salt concentration, and pH. J Clin Invest 107:317–324.
Jung DW, Apel LM, Brierley GP. 1992. Transmembrane gradients of free Na^+ in isolated heart mitochondria estimated using a fluorescent probe. Am J Physiol 262:C1047–C1055.
Jung DW, Baysal K, Brierley GP. 1995. The sodium-calcium antiport of heart mitochondria is not electroneutral. J Biol Chem 270:672–678.
Kapus A, Szaszi K, Kaldi K, Ligeti E, Fonyo A. 1990. Ruthenium red inhibits mitochondrial Na^+ and K^+ uniports induced by magnesium removal. J Biol Chem 265:18063–18066.
Kirichok Y, Krapivinsky G, Clapham DE. 2004. The mitochondrial calcium uniporter is a highly selective ion channel. Nature 427:360–364.
Lei SZ, Pan ZH, Aggarwal SK, Chen HS, Hartman J, Sucher NJ, Lipton SA. 1992. Effect of nitric oxide production on the redox modulatory site of the NMDA receptor-channel complex. Neuron 8:1087–1099.
Magistretti PJ, Pellerin L, Rothman DL, Shulman RG. 1999. Energy on demand. Science 283:496–497.
Mallat S. 1989. A theory for multiresolution signal decomposition: The wavelet decomposition. IEEE Trans Pattern Anal Mach Intell 11:674–693.
Mitchell P. 1979. Keilin's respiratory chain concept and its chemiosmotic consequences. Science 206:1148–1159.
Montero M, Alonso MT, Carnicero E, Cuchillo-Ibanez I, Albillos A, Garcia AG, Garcia-Sancho J, Alvarez J. 2000. Chromaffin-cell stimulation triggers fast millimolar mitochondrial Ca^{2+} transients that modulate secretion. Nat Cell Biol 2:57–61.
Morgenthaler FD, Kraftsik R, Catsicas S, Magistretti PJ, Chatton J-Y. 2006. Glucose and lactate are equally effective in energizing activity-dependent synaptic vesicle turnover in purified cortical neurons. Neuroscience 141:157–165.
Nguyen MH, Dudycha SJ, Jafri MS. 2007. The effects of Ca^{2+} on cardiac mitochondrial energy production is modulated by Na^+ and H^+ dynamics. Am J Physiol Cell Physiol 292:C2004–C2020.
Nicholls DG, Budd SL. 2000. Mitochondria and neuronal survival. Physiol Rev 80:315–360.
Parri HR, Gould TM, Crunelli V. 2001. Spontaneous astrocytic Ca^{2+} oscillations in situ drive NMDAR-mediated neuronal excitation. Nat Neurosci 4:803–812.
Pawelczyk T, Olson MS. 1995. Changes in the structure of pyruvate dehydrogenase complex induced by mono- and divalent ions. Int J Biochem Cell Biol 27:513–521.
Pinton P, Rimessi A, Romagnoli A, Prandini A, Rizzuto R. 2007. Biosensors for the detection of calcium and pH. Methods Cell Biol 80:297–325.
Pivovarova NB, Pozzo-Miller LD, Hongpaisan J, Andrews SB. 2002. Correlated calcium uptake and release by mitochondria and endoplasmic reticulum of CA3 hippocampal dendrites after afferent synaptic stimulation. J Neurosci 22:10653–10661.
Putney LK, Denker SP, Barber DL. 2002. The changing face of the Na^+/H^+ exchanger, NHE1: structure, regulation, and cellular actions. Annu Rev Pharmacol Toxicol 42:527–552.
Reynolds IJ, Rintoul GL. 2004. Mitochondrial stop and go: Signals that regulate organelle movement. Sci STKE 2004:PE46.
Rizzuto R, Pinton P, Carrington W, Fay FS, Fogarty KE, Lifshitz LM, Tuft RA, Pozzan T. 1998. Close contacts with the endoplasmic reticulum as determinants of mitochondrial Ca^{2+} response. Science 280: 1763–1766.
Sorg O, Magistretti PJ. 1992. Vasoactive intestinal peptide and noradrenaline exert long-term control on glycogen levels in astrocytes: Blockade by protein synthesis inhibition. J Neurosci 12: 4923–4931.
Ubl JJ, Chatton J-Y, Chen S, Stucki JW. 1996. A critical evaluation of in situ measurement of mitochondrial electrical potentials in single hepatocytes. Biochim Biophys Acta 1276:124–132.
Unser M, Aldroubi A. 1996. A review of wavelets in biomedical applications. Proc IEEE 84:626–638.
Unser M, Blu T. 2000. Fractional splines and wavelets. SIAM Rev 42:43–67.
Wakabayashi S, Hisamitsu T, Pang T, Shigekawa M. 2003. Kinetic dissection of two distinct proton binding sites in Na^+/H^+ exchangers by measurement of reverse mode reaction. J Biol Chem 278:43580–43585.
Walter L, Hajnoczky G. 2005. Mitochondria and endoplasmic reticulum: The lethal interorganelle cross-talk. J Bioenerg Biomembr 37:191–206.
Yang KT, Pan SF, Chien CL, Hsu SM, Tseng YZ, Wang SM, Wu ML. 2004. Mitochondrial Na^+ overload is caused by oxidative stress and leads to activation of the caspase 3-dependent apoptotic machinery. FASEB J 18:1442–1444.